

A Jointly Design for STAR-RIS enhanced NOMA-CoMP Networks: A Simultaneously- Signal-Enhancement-and-Cancellation-based (SSECB) Design

Tianwei Hou, *Member, IEEE*, Jun Wang, Yuanwei Liu, *Senior Member, IEEE*,
Xin Sun,
Anna Li and Bo Ai, *Senior Member, IEEE*,

Abstract

In this letter, a novel simultaneously transmitting and reflecting (STAR) reconfigurable intelligent surfaces (RISs) design is proposed in a non-orthogonal multiple access (NOMA) enhanced coordinated multi-point transmission (CoMP) network. Based on the insights of signal-enhancement-based (SEB) and signal-cancellation-based (SCB) designs, we propose a novel simultaneously-signal-enhancement-and-cancellation-based (SSECB) design, where the inter-cell interferences and desired signals can be simultaneously eliminated and boosted. Our simulation results demonstrate that: i) the inter-cell interference can be perfectly eliminated, and the desired signals can be enhanced simultaneously with the aid of a large number of RIS elements; ii) the proposed SSECB design is capable of outperforming the conventional SEB and SCB designs.

Index Terms

CoMP, NOMA, STAR-RIS, SSECB.

This work is supported by the National Natural Science Foundation of China under Grant 61901027. (Corresponding author: Anna Li.)

T. Hou, J. Wang, X. Sun, B. Ai are with the School of Electronic and Information Engineering, Beijing Jiaotong University, Beijing 100044, China ({email: twhou, wangjun1, xsun, boai}@bjtu.edu.cn).

Y. Liu and Anna Li are with School of Electronic Engineering and Computer Science, Queen Mary University of London, London E1 4NS, U.K. (e-mail: yuanwei.liu@qmul.ac.uk, A.li@qmul.ac.uk).

I. INTRODUCTION

Reconfigurable intelligent surfaces (RISs) stand as a potential solution of spectral efficiency (SE) enhancement and coverage enhancement for the sixth-generation (6G) wireless networks [1], [2]. By properly controlling both the phase shift and even the amplitude of these RIS elements, the received signals can be beneficially boosted or mitigated. Recently, by considering both the transmission and reflection of the RIS elements, a novel concept of simultaneous transmitting and reflecting RISs (STAR-RISs) attracts considerable attention, where the incident wireless signals can be reflected within the half-space at the same side of the RIS, but they can also be transmitted into the other side of the RIS [3], [4].

In practice, the coordinated multi-point transmission (CoMP) technique is adopted in the third generation partnership project (3GPP) for cellular networks, where the SE and energy efficiency (EE) is limited by the impacts of inter-cell interferences [5]. The scarce of SE and EE in 6G has stimulated the development of advanced multiple access techniques, i.e., non-orthogonal multiple access (NOMA) [6]. One of the main direction of the NOMA-CoMP networks, namely NOMA-coordinated-beamforming (CB), received considerable attention [7]. In NOMA-CB, the cell-edge user (CEU) and cell-center user (CCU) are served by its desired BS, where zero-forcing based design was proposed for mitigating the intra-cell and inter-cell interferences by sacrificing the spatial diversity gain of the desired links [8], which motivates us to employ RIS for the NOMA-CoMP networks.

By considering the application of the reflected signals at the RIS elements, a pair of main directions of the RIS enhanced networks were proposed, namely signal-enhancement-based (SEB) and signal-cancellation-based (SCB) designs [9]. By assuming that multiple waves are co-phase at the receivers, the received signal can be significantly boosted [10]. In contrast, another reason for implementing RISs is to align the reflected signals for signal cancellation [11]. However, previous contributions mainly focus on the SEB-only or SCB-only designs, whilst there is a paucity of investigations on the simultaneously-signal-enhancement-and-cancellation-based (SSECB) design. Fortunately, with the aid of the STAR-RIS, the SSECB designs become possible for implementing NOMA-CoMP networks.

However, as mentioned above, there are still many challenges of STAR-RIS enhanced NOMA-CoMP networks. For example, on the one hand, the passive beamforming design of STAR-RIS

for the SSECB design is still an open issue. On the other hand, the minimal required number of RIS elements is also worth estimating. Hence, in order to provide the benchmark scheme of the STAR-RIS enhanced NOMA-CoMP networks, we propose a novel SSECB design, which provides the desired degree of flexibility for the STAR-RIS enhanced networks. Our contributions can be summarized as follows:

- We first propose a novel RIS enhanced CoMP network by NOMA-CB, where each BS serves its own users and RIS array. By assuming that each STAR-RIS elements are capable of both transmitting and reflecting the incident signals, the signals can be controlled in full-spaces.
- We then propose a novel SSECB design in the STAR-RIS enhanced NOMA-CoMP networks, where the inter-cell interference can be eliminated by the transmission of the STAR-RIS elements for enhancing the network's performance, whereas the remaining signals can be reflected to its desired users. The minimal required number of RIS elements is derived in the case of strong-line-of-sight (LoS) links.
- Our simulation results illustrate that 1) The minimal required number of RIS elements is mainly impacted by the distances and path-loss exponent of the interference and transmission links; 2) Since the small-scale fading gains are random variables, the inter-cell interference can be cancelled perfectly in the case that the number of RIS elements is large enough; 2) The proposed SSECB design is capable of outperforming the conventional SEB and SCB designs.

II. SYSTEM MODEL

The system model of the STAR-RIS enhanced NOMA-CoMP networks is illustrated in Fig. 1, where two cells are deployed for serving the CCUs and CEUs simultaneously in downlink. The BSs equipped with a single transmitting antenna is communicating with one CCU and one CEU each equipped with a single receiving antenna by utilizing the power-domain NOMA techniques.

Without loss of generality, it is assumed that the BS located in cell1 is BS1, and the users located in cell1 treat the signals received from BS2 as interferences, whereas the users located in cell1 treat the signals received from BS1 as desired signals. The CCU and CEU located in cell1 are denoted by CCU1 and CEU1, respectively.

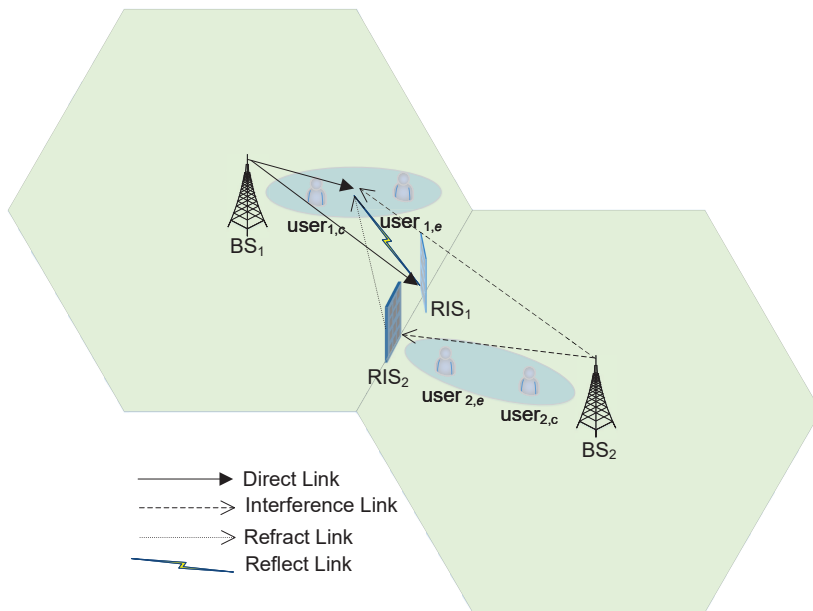


Fig. 1: System model of the STAR-RIS enhanced NOMA-CoMP networks.

In this letter, there are two RIS arrays located at the intersection of two cells, each of which is employed with L RIS elements with $L \geq 1$ for implementing the proposed CoMP communications. In this Section, by properly controlling the transmission and reflection amplitude coefficients and phase shifts of each RIS element, both the desired and interference signals can be beneficially enhanced and mitigated, respectively. Note that \mathbf{H}^T and \mathbf{H}^H denote the transpose and conjugate transpose of the matrix \mathbf{H} in the rest of this letter.

A. System Description of STAR-RIS enhanced NOMA-CoMP Networks

Due to the strong scattering effect of the BS-user links, the small-scale fading between BS1 and CCU1, which is the desired link, can be modelled by Rayleigh fading channel $w_{1,1,c}$. Note that the probability density function (PDF) of the Rayleigh fading channel gains is given by

$$f(x) = e^{-x}. \quad (1)$$

In this letter, we only focus on the impact of the path-loss, and hence the large-scale fading of the desired links for CCU1 in BS1 can be considered as Non-LoS (NLoS) link, which is given

by

$$\varepsilon_{1,1,c} = d_{1,1,c}^{-\alpha_1}, \quad (2)$$

where α_1 denotes the path-loss exponent of the desired link, $d_{1,1,c}$ denotes the distance of the BS1-CCU1 links.

In practice, the users located in BS1 also detect the signals from BS2, which can be modelled by

$$I = w_{2,1,c} d_{2,1,c}^{-\alpha_4}, \quad (3)$$

where α_4 denotes the path-loss exponent of the interference link, $d_{2,1,c}$ and $w_{2,1,c}$ denote the distance and small-scale fading gain of the BS2-CCU1 links, respectively. Note that the small-scale fading gain of the interference links also modelled by Rayleigh fading channel.

In the proposed CoMP networks, for simplicity, we consider that one RIS arrays and one BS are grouped, where RIS arrays 1 and 2 face to the selected BS1 and BS2, respectively. The Rician fading channels are adopted for modelling the LoS of the BS1-RIS1 links as follows:

$$\mathbf{H}_1 = \begin{bmatrix} h_{1,R,1} \\ \vdots \\ h_{1,R,L} \end{bmatrix}, \quad (4)$$

where \mathbf{H}_i is a $(L \times 1)$ vector containing Rician fading channel gains, which is given by

$$h_{1,R,l} = \sqrt{\frac{\mathcal{K}_1}{\mathcal{K}_1 + 1}} h_{1,R,l}^{\text{LoS}} + \sqrt{\frac{1}{\mathcal{K}_1 + 1}} h_{1,R,l}^{\text{NLoS}}, \quad (5)$$

where \mathcal{K}_1 denotes the Rician factor of the BS-RIS link. $h_{1,R,l}^{\text{LoS}}$ and $h_{1,R,l}^{\text{NLoS}}$ denote the LoS and NLoS components, respectively.

On the one hand, the RIS elements are capable of reflecting the received signals to the users. Hence, similar to (4), the small-scale fading vector of the reflected links, i.e., RIS1-CCU1, is defined by

$$\mathbf{R}_{1,c} = \begin{bmatrix} r_{1,c,1} & \cdots & r_{1,c,L} \end{bmatrix}, \quad (6)$$

where $\mathbf{R}_{1,c}$ is $(1 \times L)$ matrix whose elements represent Rician fading channel gains with fading

parameter \mathcal{K}_2 . Similarly, the channel gains of the RIS-user link is given by

$$r_{l,c,l} = \sqrt{\frac{\mathcal{K}_2}{\mathcal{K}_2 + 1}} r_{1,c,l}^{\text{LoS}} + \sqrt{\frac{1}{\mathcal{K}_2 + 1}} r_{1,c,l}^{\text{NLoS}}, \quad (7)$$

where $r_{1,c,l}^{\text{LoS}}$ and $r_{1,c,l}^{\text{NLoS}}$ denote the LoS and NLoS components, respectively.

The RIS arrays are co-located at the intersection of two cells, and hence the large-scale fading channels of the BS1-RIS1 and RIS1-CCU1 can be considered as LoS links, which is given by

$$\varepsilon_{1,R,c} = d_{1,R}^{-\alpha_2} d_{R,1,c}^{-\alpha_3}, \quad (8)$$

where $d_{1,R}$ denotes the distance of the BS1-RIS1, $d_{R,1,c}$ denotes the distance of the RIS1-CCU1, α_2 and α_3 denote the path-loss exponents of the BS-RIS and RIS-user links.

On the other hand, the RIS elements are also capable of transmitting the received signals to the users located in the nearby cells. Hence, RIS1 transmits the signal to the users located in cell2, and the small-scale fading vector of the RIS1-CCU2 links can be defined by

$$\mathbf{T}_{1,2,c} = \left[t_{1,2,c,1}, \dots, t_{1,2,c,L} \right], \quad (9)$$

where $\mathbf{T}_{1,2,c}$ is $(1 \times L)$ matrix whose elements represent Rician fading channel gains with fading parameter \mathcal{K}_3 , which can be written as

$$t_{1,2,c,l} = \sqrt{\frac{\mathcal{K}_3}{\mathcal{K}_3 + 1}} t_{1,2,c,l}^{\text{LoS}} + \sqrt{\frac{1}{\mathcal{K}_3 + 1}} t_{1,2,c,l}^{\text{NLoS}}, \quad (10)$$

where $t_{1,2,c,l}^{\text{LoS}}$ and $t_{1,2,c,l}^{\text{NLoS}}$ denote the LoS and NLoS components, respectively. Similarly, the large-scale fading of the BS1-RIS1-CCU2 is defined by

$$\varepsilon_{1,T,c} = d_{1,R}^{-\alpha_2} d_{R,2,c}^{-\alpha_3}, \quad (11)$$

where $d_{R,2,c}$ represents the distance of the RIS1-CCU2 links.

B. Jointly Beamforming Designs

In order to simultaneously control multiple RIS elements, and to implement the proposed SSECB design, as well as based on the maturity of low-complexity channel estimation algorithms [12], [13], the global CSIs are assumed to be perfectly known at the RIS controller.

Without loss of generality, we focus on the CCU1, and the received signals at CCU1 is given

by

$$\begin{aligned}
y_{1,c} = & \underbrace{\sqrt{\varepsilon_{1,1,c}}w_{1,1,c}p + \sqrt{\varepsilon_{1,R,c}}\mathbf{R}_{1,1,c}\mathbf{\Phi}_{1,R}\mathbf{H}_1p}_{\text{Desired Signal}} \\
& + \underbrace{\sqrt{\varepsilon_{2,1,c}}w_{2,1,c}p + \sqrt{\varepsilon_{1,T,c}}\mathbf{T}_{1,2,c}\mathbf{\Phi}_{2,T}\mathbf{H}_2p}_{\text{Interference}} + N_0,
\end{aligned} \tag{12}$$

where p denotes the transmit power at the BS, $\mathbf{\Phi}_{2,T} \triangleq \text{diag} [\beta_{2,T,1}\phi_{2,T,1}, \beta_{2,T,2}\phi_{2,T,2}, \dots, \beta_{2,T,L}\phi_{2,T,L}]$ denotes both the transmitting phase shifts and transmitting amplitude coefficients of the 2-nd RIS array. More specifically, $\beta_{2,T,l} \in (0, 1]$ denotes the transmission amplitude coefficient of RIS element l in the 2-nd RIS array, $\phi_{2,T,l} = \exp(j\theta_{2,T,l}), j = \sqrt{-1}, \forall l = 1, 2 \dots, L$. $\theta_l \in [0, 2\pi)$ denotes the transmitting phase shift by RIS element l in the 2-nd RIS array. Similarly, $\mathbf{\Phi}_{1,R} \triangleq \text{diag} [\beta_{1,R,1}\phi_{1,R,1}, \dots, \beta_{1,R,L}\phi_{1,R,L}]$ represents the reflection phase shifts and reflection amplitude coefficients of the 1-st RIS array. The additive white Gaussian noise (AWGN) is denoted by N_0 with variance σ^2 .

Based on the insights from [3], [4], there is one obvious constraint on the reflection and transmission amplitude coefficients, which can be written as:

$$\beta_{1,R,l}^2 + \beta_{1,T,l}^2 \leq 1. \tag{13}$$

For simplicity, it is assumed that $\beta_{1,R,l}^2 + \beta_{1,T,l}^2 = 1$ in the rest of this letter.

In order to simultaneously accomplish signal enhancement and cancellation goals, the passive beamforming at two RIS arrays must be designed jointly. We first focus our attention on cell1, and hence the design of the transmission at the 2-nd RIS array is to mitigate the inter-cell interference of the users in cell1, which can be expressed as follows:

$$\begin{aligned}
& \min \sqrt{\varepsilon_{2,1,c}}w_{2,1,c}p + \sqrt{\varepsilon_{2,T,c}}\mathbf{T}_{2,1,c}\mathbf{\Phi}_{2,T}\mathbf{H}_2p, \\
& \min \sqrt{\varepsilon_{2,1,e}}w_{2,1,e}p + \sqrt{\varepsilon_{2,T,e}}\mathbf{T}_{2,1,e}\mathbf{\Phi}_{2,T}\mathbf{H}_2p, \\
& \text{Subject to } \beta_{2,T,l} \leq 1, \forall l=1 \dots L, \\
& \phi_{2,T,l}, \dots, \phi_{2,T,l} \in [0, 2\pi).
\end{aligned} \tag{14}$$

In order to achieve the ambitious objective in (14), we first generate the effective transmission

channel gain of the BS2-RIS2-CCU1 and BS2-RIS2-CEU1 links as follows:

$$\overline{\mathbf{H}}_{2,T} = \begin{bmatrix} h_{2,R,1}t_{2,1,c,1} & \cdots & h_{2,R,L}t_{2,1,c,L} \\ h_{2,R,1}t_{2,1,e,1} & \cdots & h_{2,R,L}t_{2,1,e,L} \end{bmatrix}. \quad (15)$$

Then, the diagonal matrix $\Phi_{2,T}$ is transformed into a vector as follows:

$$\overline{\Phi}_{2,T} = [\beta_{2,T,1}\phi_{2,T,1}, \cdots, \beta_{2,T,L}\phi_{2,T,L}]^T. \quad (16)$$

We then turn our attention to the passive beamforming design at the 2-nd RIS array, where the transmission phase shifts and transmission amplitude coefficients are jointly manipulated. Therefore, the objective in (14) can be rewritten as

$$\overline{\mathbf{H}}_{2,T}\overline{\Phi}_{2,T} = \mathbf{I}_{2,1}, \quad (17)$$

where $\mathbf{I}_{2,1}$ is a 2×1 vector, which represents the received inter-cell interference at CCU1 and CCU2 with $\mathbf{I}_{2,1} = \begin{bmatrix} -\sqrt{\frac{\varepsilon_{2,1,c}}{\varepsilon_{2,T,c}}}w_{2,1,c} \\ -\sqrt{\frac{\varepsilon_{2,1,e}}{\varepsilon_{2,T,e}}}w_{2,1,e} \end{bmatrix}$. Thus, the transmission phase shifts and transmission amplitude coefficients can be readily obtained by

$$\overline{\Phi}_{2,T} = \overline{\mathbf{H}}_{2,T}^{-1}\mathbf{I}_{2,1}. \quad (18)$$

Similarly, the 1-st RIS transmits the signal received from BS1 to the users located in cell2 for interference cancellation, and hence the rest of power can be reflected to the CCU1 for signal enhancement. Then, the reflection phase shifts and reflection amplitude coefficients at the 1-st RIS can be given by

$$\overline{\Phi}_{1,R} = [\beta_{1,R,1}\phi_{1,R,1}, \cdots, \beta_{1,R,L}\phi_{1,R,L}]^T, \quad (19)$$

where $\phi_{1,R,l}$ denotes the reflection phase shifts at the l -th RIS element of the 1-st RIS. It is commonly assumed that the transmission and reflection phase shifts at RIS elements are independent [3], [4]. Thus, the reflection of the RIS is to maximal the received power at the

CCU, and the objective can be given by

$$\begin{aligned} & \max \sqrt{\varepsilon_{1,1,c}} w_{1,1,c} p + \sqrt{\varepsilon_{1,R,c}} \mathbf{R}_{1,1,c} \mathbf{\Phi}_{1,R} \mathbf{H}_1 p, \\ & \text{Subject to } \beta_{1,R,l} \leq 1, \forall l=1 \cdots L, \\ & \quad \phi_{1,R,l}, \cdots, \phi_{1,R,l} \in [0, 2\pi), \end{aligned} \quad (20)$$

where $\varepsilon_{1,1,c} = d_{1,1,c}^{-\alpha_1}$ and $\varepsilon_{1,R,c} = d_{1,R}^{-\alpha_2} d_{R,1,c}^{-\alpha_3}$ represent the large-scale fading of the BS1-CCU1 and the BS1-RIS1-CCU1 links, respectively. $w_{1,1,c}$ and $\mathbf{R}_{1,1,c}$ denote the small-scale channel gains of BS1-CCU1 and RIS1-CCU1, respectively. $\mathbf{\Phi}_{1,R}$ denotes the reflection diagonal matrix of the RIS1.

To solve the objective in (20), we then generate a reflection vector of the 1-st RIS array as follows:

$$\overline{\mathbf{H}}_{1,R,c} = \begin{bmatrix} h_{1,R,1} r_{1,c,1} & \cdots & h_{1,R,L} r_{1,c,L} \end{bmatrix}. \quad (21)$$

Then, the reflection phase shift of the 1-st RIS array can be obtained as:

$$\tilde{\mathbf{\Phi}}_{1,R}^T = \arg(\overline{\mathbf{H}}_{1,R,c}) - \arg(w_{1,1,c}), \quad (22)$$

where $\arg(\cdot)$ denotes the angle function. By doing so, the received signals from the BS1-CCU1 and BS1-RIS1-CCU1 can be coherently boosted, and thus the channel gain is given by

$$|h|_{1,1,c} = \sqrt{\varepsilon_{1,R,c}} \sum_{l=1}^L |h_{1,R,l} r_{1,c,l} \beta_{1,R,l}| + \sqrt{\varepsilon_{1,1,c}} |w_{1,1,c}|. \quad (23)$$

Based on the upon jointly passive beamforming designs in (18) and (22) at two STAR-RIS arrays, the proposed SSECB design can be achieved, where the desired signals can be enhanced, while the interference signals can be cancelled simultaneously. Hence, the signal-to-interference-plus-noise-ratio (SINR) of the CEU1 can be written as

$$SINR_{1,e} = \frac{|h|_{1,1,e}^2 p \alpha_e^2}{|h|_{1,1,e}^2 p \alpha_c^2 + \rho^2}, \quad (24)$$

where α_e^2 and α_c^2 denote the power allocation factors of the CEU and CCU with $\alpha_e^2 + \alpha_c^2 = 1$, respectively. Since the reflection at the RIS mainly focuses on the signal enhancement for the CCUs, the signals received at the CEUs are superimposed, and hence the channel gain of CEU1

can be given by $|h|_{1,1,e} = \left| \sqrt{\varepsilon_{1,R,e}} \sum_{l=1}^L h_{1,R,l} r_{1,e,l} \beta_{1,R,l} + \sqrt{\varepsilon_{1,1,e}} w_{1,1,e} \right|$.

Based on the application of the SIC technique at the CCUs, who first detect the signal of the CEU with the following SINR:

$$SINR_{1,e \rightarrow 1,c} = \frac{|h|_{1,1,c}^2 p \alpha_e^2}{|h|_{1,1,c}^2 p \alpha_c^2 + \rho^2}, \quad (25)$$

Then the CCUs can detect its own signal with the following signal-to-noise-ratio (SNR):

$$SNR_{1,c} = \frac{|h|_{1,1,c}^2 p \alpha_c^2}{\rho^2}. \quad (26)$$

Remark 1. For simplicity, it is assumed that the channels are in the strong LoS scenario, where all channel gains are one. Based on the proposed SSECB design in (18), and in order to mitigate inter-cell interferences at both the CCUs and CEUs, the following constraints on the number of RIS elements need to be met:

$$L > \max \left\{ \sqrt{\frac{\varepsilon_{2,1,c}}{\varepsilon_{2,T,c}}}, \sqrt{\frac{\varepsilon_{2,1,e}}{\varepsilon_{2,T,e}}} \right\}, \quad (27)$$

otherwise no solution exists.

Thus, the achievable rate of the CCU and CEU can be obtained by:

$$R_{1,c} = \mathbb{E} \{ \log_2 (1 + SNR_{1,c}) \}, \quad (28)$$

and

$$R_{1,e} = \mathbb{E} \{ \log_2 (1 + SINR_{1,e}) \}, \quad (29)$$

where $\mathbb{E}\{\}$ represents the expectation function.

III. NUMERICAL RESULTS

In this section, numerical results are provided for the performance evaluation of the proposed SSECB design in the STAR-RIS enhanced NOMA-CoMP networks. The transmission bandwidth of the proposed network is set to $B = 1$ MHz, and the power of the AWGN is set to $\rho^2 = -174 + 10 \log_{10}(B)$ dBm. Based on NOMA protocol, the paired users share the power with the power allocation factors $\alpha_e^2 = 0.6$ and $\alpha_c^2 = 0.4$. Some detailed parameters are illustrated in Table I.

TABLE I: SIMULATION PARAMETERS

The distances of the BS1-CCU1 and BS2-CCU2	30 m
The distances of the BS1-CEU1 and BS2-CEU2	60 m
The distances of the BS1-RIS1 and BS2-RIS2	70 m
The distances of the RIS1-CEU1 and RIS2-CEU2	15 m
The distances of the RIS1-CCU1 and RIS2-CCU2	50 m
The distances of the BS1-CCU2 and BS2-CCU1	120 m
The distances of the BS1-CEU2 and BS2-CEU1	90 m
The path-loss exponent of BS-user links	$\alpha_1 = 3$
The path-loss exponent of BS-RIS links	$\alpha_2 = 2.8$
The path-loss exponent of RIS-CEU links	$\alpha_3 = 2.5$
The path-loss exponent of RIS-CCU links	$\alpha_3 = 2.8$
The path-loss exponent of interference links	$\alpha_4 = 3.5$
The fading parameters	$\hat{\mathcal{K}}_2 = 2 \hat{\mathcal{K}}_3 = 3$

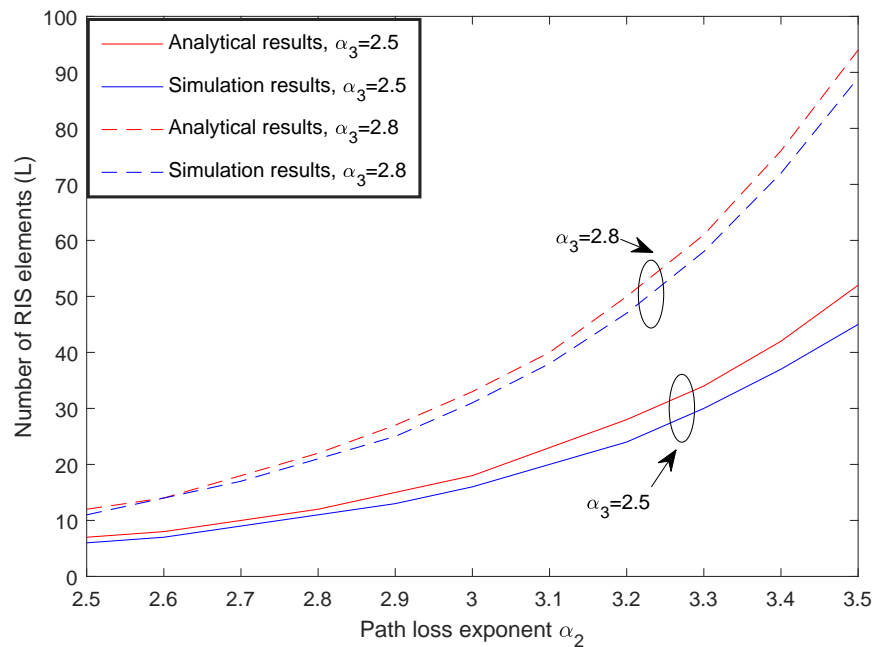


Fig. 2: Minimal required number of RIS elements for the proposed SSECB design in the STAR-RIS enhanced NOMA-CoMP networks, where the small-scale channel gains are normalized to all one.

1) *Minimal Required Number of RIS elements:* In Fig. 2, we evaluate the minimal required number of RIS elements of each RIS array for implementing the proposed SSECB design. Observe that as the path loss exponent increases, the minimal required number of RIS elements increases, which indicates that the path-loss exponent of the BS-RIS and RIS-user links are required to be higher than that of the interference links of the proposed SSECB design. Further-

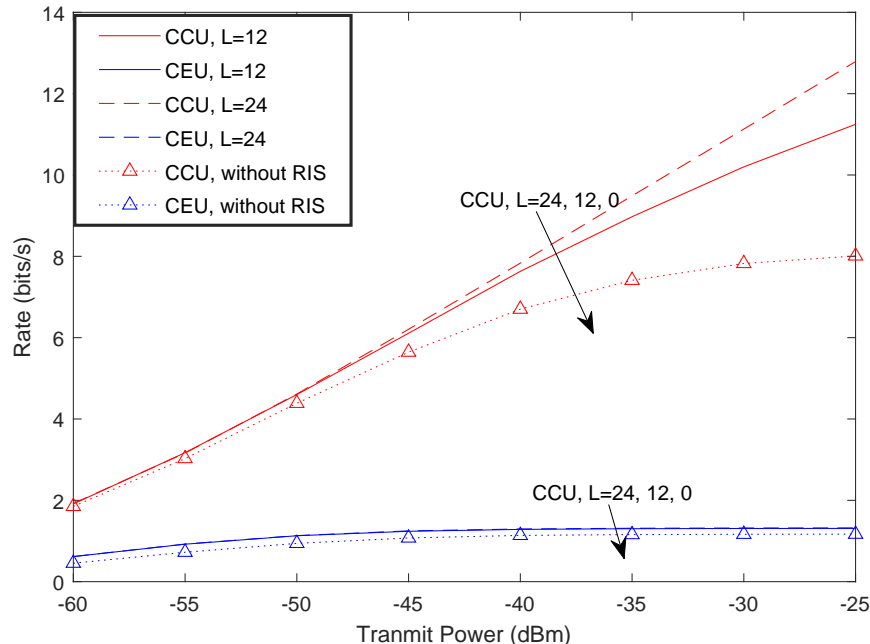


Fig. 3: The achievable rate of both the CCU and CEU versus the transmit power with different number of RIS elements. The minimal number of RIS element is obtained to $L = 12$ for the selected parameters.

more, note that in the simulation results, it is also assumed that the small-scale channel gains are also normalized to one for simplicity, and hence, the number of RIS elements should be greater than the minimal number of RIS elements in practice.

2) *Impact of the Number of RIS Elements:* In Fig. 3, we evaluate the achievable rate of both the CCU and CEU in the proposed SSECB design. The number of RIS elements is obtained by (27), where $L = 12$ in the case of the selected parameter setting. By comparing the red solid curve and dashed curve, we can see that in the case of $L = 24$, which is two times of the minimal required number of RIS elements, the high-SNR slope of the achievable rate is one, which illustrates that the interferences received from nearby cells are mitigated perfectly. One can also observe that the achievable rate ceilings occur in the case of $L = 12$, which is due to the fact that the number of RIS elements is not enough for interference cancellation, and hence the inter-cell interference residue exists. Observe that the performance gap between the proposed SSECB design and the case without RIS increases, which also illustrates the superiority of the proposed SSECB design.

3) *Impact of Different Passive Beamforming Designs:* In Fig. 4, we evaluate the achievable

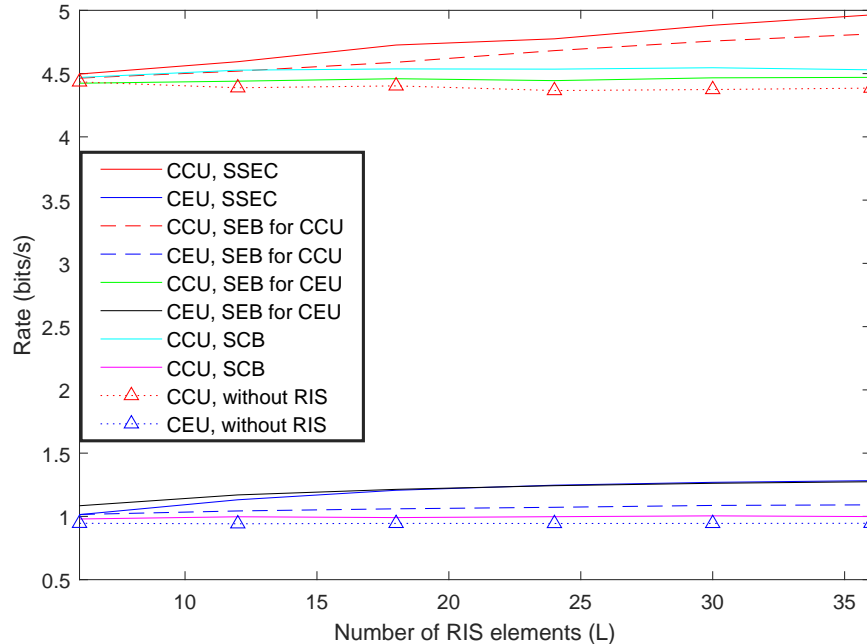


Fig. 4: The achievable rate of both the CCU and CEU versus the number of RIS elements with different passive beamforming designs. The transmit power of the BS is set to $p = -50$ dBm.

rate of the paired NOMA users with different passive beamforming at RIS elements. By aligning the reflected signals and desired signal perfect coherent at the CCU or CEU, the dashed, green and black curves are obtained for comparing the performance of a pair of SEB designs. We can see that the achievable rate of the proposed SSECB design is higher than other benchmark schemes, which illustrate that the proposed SSECB design is capable of outperforming the other SEB and SEC designs.

IV. CONCLUSIONS

In this letter, we first reviewed previous contributions related to the RIS-enhanced SEB and SCB designs, and we then utilized a novel STAR-RIS for the proposed SSECB design. In order to provide a practical design of the STAR-RIS enhanced NOMA-CoMP networks, we designed a jointly passive beamforming weight, where the transmission and reflection of RIS elements are used for inter-cell interference cancellation and signal enhancement, respectively. Compared to the previous SEB and SCB designs, the proposed STAR-RIS enhanced SSECB design has superior performance on achievable rate. An important future direction is to add more TA and

RA at the BS and users by jointly designing both the active beamforming, passive beamforming, and detection vectors.

REFERENCES

- [1] M. D. Renzo, A. Zappone, M. Debbah, M.-S. Alouini, C. Yuen, J. de Rosny, and S. Tretyakov, "Smart radio environments empowered by reconfigurable intelligent surfaces: How it works, state of research, and road ahead," *IEEE J. Sel. Areas Commun.*, vol. 38, no. 11, pp. 2450–2525, Nov. 2020.
- [2] Q. Wu and R. Zhang, "Towards smart and reconfigurable environment: Intelligent reflecting surface aided wireless network," *IEEE Commun. Mag.*, vol. 58, no. 1, pp. 106–112, Jan. 2020.
- [3] Y. Liu, X. Mu, J. Xu, R. Schober, Y. Hao, H. V. Poor, and L. Hanzo, "STAR: Simultaneous transmission and reflection for 360° coverage by intelligent surfaces," *Arxiv*, vol. 2103.09104v2, pp. 1–1, Mar. 2021.
- [4] J. Xu, Y. Liu, X. Mu, and O. A. Dobre, "STAR-RISs: Simultaneous transmitting and reflecting reconfigurable intelligent surfaces," *Arxiv*, vol. 2101.09663v2, pp. 1–1, Mar. 2021.
- [5] 3GPP TR 36.819 V11.0.0, "Coordinated multi-point operation for LTE," Sep. 2011.
- [6] Z. Ding, Y. Liu, J. Choi, Q. Sun, M. Elkashlan, C. L. I, and H. V. Poor, "Application of non-orthogonal multiple access in LTE and 5G networks," *IEEE Commun. Mag.*, vol. 55, no. 2, pp. 185–191, Feb. 2017.
- [7] W. Shin, M. Vaezi, B. Lee, D. J. Love, J. Lee, and H. V. Poor, "Non-orthogonal multiple access in multi-cell networks: Theory, performance, and practical challenges," *IEEE Commun. Mag.*, vol. 55, no. 10, pp. 176–183, 2017.
- [8] W. Shin *et al.*, "Coordinated beamforming for multi-cell MIMO-NOMA," *IEEE Commun. Lett.*, vol. 21, no. 1, pp. 84–87, 2017.
- [9] Y. Liu, X. Liu, X. Mu, T. Hou, J. Xu, Z. Qin, M. D. Renzo, and N. Al-Dhahir, "Reconfigurable intelligent surfaces: Principles and opportunities," *Arxiv*, vol. 2007.03435v2, pp. 1–1, 2021.
- [10] T. Hou, Y. Liu, Z. Song, X. Sun, Y. Chen, and L. Hanzo, "Reconfigurable intelligent surface aided NOMA networks," *IEEE J. Sel. Areas Commun.*, vol. 38, no. 11, pp. 2575–2588, Nov. 2020.
- [11] T. Hou, Y. Liu, Z. Song, X. Sun, and Y. Chen, "MIMO-NOMA networks relying on reconfigurable intelligent surface: A signal cancellation-based design," *IEEE Trans. Commun.*, vol. 68, no. 11, pp. 6932–6944, Nov. 2020.
- [12] Q. Wu and R. Zhang, "Beamforming optimization for wireless network aided by intelligent reflecting surface with discrete phase shifts," *IEEE Trans. Commun.*, vol. 68, no. 3, pp. 1838–1851, Mar. 2020.
- [13] Z. Wan, Z. Gao, and M.-S. Alouini, "Broadband channel estimation for intelligent reflecting surface aided mmwave massive MIMO systems," *Arxiv*, vol. 2002.01629v1, pp. 1–1, Feb. 2020.